3-2009

Dimer-Dimer Collisions at Finite Energies in Two-Component Fermi Gases

J P. D'Incao

Seth T. Rittenhouse

Nirav P. Mehta
Trinity University, nmehta@trinity.edu

Chris H. Greene

PHYSICAL REVIEW A **79**, 030501(R) (2009)

Dimer-dimer collisions at finite energies in two-component Fermi gases

J. P. D'Incao, Seth T. Rittenhouse, N. P. Mehta,* and Chris H. Greene
Department of Physics and JILA, University of Colorado, Boulder, Colorado 80309-0440, USA
(Received 18 June 2008; published 11 March 2009)

We discuss a major theoretical generalization of existing techniques for handling the three-body problem that accurately describes the interactions among four fermionic atoms. Application to a two-component Fermi gas accurately determines dimer-dimer scattering parameters at finite energies and can give deeper insight into the corresponding many-body phenomena. To account for finite temperature effects, we calculate the energy-dependent *complex* dimer-dimer scattering length, which includes contributions from elastic and inelastic collisions. Our results indicate that strong finite-energy effects and dimer dissociation are crucial for understanding the physics in the strongly interacting regime for typical experimental conditions. While our results for dimer-dimer relaxation are consistent with experiment, they confirm only partially a previously published theoretical result.

DOI: 10.1103/PhysRevA.79.030501 PACS number(s): 31.15.xj, 34.50.Cx, 67.85.−d

The physics of strongly interacting fermionic systems is of fundamental importance in many areas of physics encompassing condensed matter physics, nuclear physics, particle physics, and astrophysics. The last few years have seen extensive theoretical and experimental efforts devoted to the field of ultracold atomic Fermi gases. The ability to control interatomic interactions through magnetically tunable Feshbach resonances has opened up broad vistas of experimentally accessible phenomena, providing a quantum playground for studying the strongly interacting regime. For instance, near a Feshbach resonance between two dissimilar fermions, the s-wave scattering length a can assume positive and negative values, allowing for the systematic exploration of Bose-Einstein condensation (BEC) and the Bardeen-Cooper-Schrieffer (BCS) crossover regime, in which bosonic ($a>0$) and fermionic ($a<0$) types of superfluidity connect smoothly [1,2]. In this broad context, few-body correlations [3,4] play an important role in describing the dynamics of such systems. On the BEC side of the resonance ($a>0$), dissimilar fermions pair up into weakly bound bosonic dimers, and the zero (collision) energy dimer-dimer scattering length, $a_{\mathrm{dd}}(0)$, determines various experimental observables such as the molecular gas collective modes, the internal energy, and even the macroscopic spatial extent of the confined cloud [1,2]. Although a better description of the many-body behavior has emerged through the inclusion of few-body correlations, most of the current understanding of crossover physics relies on zero-energy theories, and very little is known about finite-energy effects in this regime (see Ref. [5] and references therein).

In this Rapid Communication we demonstrate important finite-energy effects which can potentially impact the physics of a finite temperature ultracold Fermi gas in the crossover regime. Our results show deviations from zero-energy dimer-dimer collisions and indicate that, at experimentally relevant temperatures and scattering lengths, molecular dissociation might play an important role. The crossover regime can be viewed as a long-lived atom-molecule mixture, where dimers are dynamically converted to atoms and vice versa. In order to account for finite temperature effects, we calculate the energy-dependent *complex* dimer-dimer scattering length, $a_{\mathrm{dd}}(E_{\mathrm{col}})$, where E_{col} is the collision energy. The real and imaginary parts of a_{dd} correspond, respectively, to contributions from elastic and inelastic (dissociative) collisions [6], both of which should be considered to properly model the Fermi gas at realistic temperatures. In the zero-energy limit we reproduce the well-known prediction $a_{\mathrm{dd}}(0)\approx 0.6a$ [4]. However, when the dimer binding energy, $E_b=\hbar^2/(2\mu_{2\mathrm{b}}a^2)$ (where $\mu_{2\mathrm{b}}$ is the two-body reduced mass) is comparable to the gas temperature T, finite-energy effects and molecular dissociation become important, defining a critical scattering length $a_c=\hbar/(2\mu_{2\mathrm{b}}k_BT)^{1/2}$, where k_B is Boltzmann's constant, beyond which an atom-molecule mixture should prevail.

We also study dimer-dimer relaxation in which two weakly bound dimers collide and make an inelastic transition to a lower-energy state. In such a process, the kinetic energy released is enough for the collision partners to escape from typical traps. Petrov *et al.* [4] predicted that, near a Feshbach resonance, dimer-dimer relaxation is suppressed as $a^{-2.55}$, explaining the long lifetimes observed in several experiments [2,7]. Here we also verify this suppression, although with an a dependence that is not described as a simple power-law scaling as originally predicted [4]. While the $a^{-2.55}$ scaling law has already been tested (Regal *et al.* [7] found $a^{-2.3\pm0.4}$ and Bourdel *et al.* [2] found $a^{-2.0\pm0.8}$), our calculations demonstrate that finite range corrections can explain the apparent experimental scaling law behavior, despite deviations from that power law for larger a.

We solve the four-body Schrödinger equation in the hyperspherical adiabatic representation, which offers a simple yet quantitative picture. A finite range model is assumed for the interatomic interaction, and a physically motivated variational basis set is adopted to solve hyperangular equations [8]. While several hyperangular parameterizations exist, we find that the best choice is the "democratic" hyperspherical coordinates [9] in which all possible fragmentation channels are treated on an equal footing, which describes elastic and inelastic processes in a unified picture.

*Present address: Department of Physics, Grinnell College 1116 8th Ave., Grinnell, IA 50112.

In the adiabatic hyperspherical representation, the collective motion of the four fermions is described in terms of the hyper-radius R, characterizing the overall size of the system. The interparticle relative motion is described by the hyperangles $\Omega \equiv \{\theta_1, \theta_2, \phi_1, \phi_2, \phi_3\}$ and the set of Euler angles $\{\alpha, \beta, \gamma\}$ specifying the orientation of the body-fixed frame [9]. θ_1 and θ_2 parametrize the moments of inertia while ϕ_1, ϕ_2, and ϕ_3 parametrize internal configurations [9]. Integrating out the hyperangular degrees of freedom, the Schrödinger equation reduces to a system of coupled ordinary differential equations given in atomic units (used throughout this Rapid Communication) by

$$\left[-\frac{1}{2\mu}\frac{d^2}{dR^2} - E\right]F_\nu(R) + \sum_{\nu'} W_{\nu\nu'}(R)F_{\nu'}(R) = 0, \qquad (1)$$

where $\mu = m/4^{1/3}$ is the four-body reduced mass (m being the atomic mass), E is the total energy, F_ν is the hyper-radial wave function, and ν represents all quantum numbers needed to label each channel. Scattering observables can then be extracted by solving Eq. (1), where the nonadiabatic couplings $W_{\nu\neq\nu'}$ drive inelastic transitions between channels described by the effective potentials $W_{\nu\nu}$.

In the hyperspherical representation, the major reduction to Eq. (1) is accomplished by finding eigenfunctions of the (fixed R) adiabatic Hamiltonian

$$\hat{H}_{\rm ad}(R,\Omega) = \frac{\hat{\Lambda}^2(\Omega) + 12}{2\mu R^2} + \hat{V}(R,\Omega). \qquad (2)$$

In the above equation, $\hat{\Lambda}$ is the grand angular momentum operator [9] and $\hat{V}$ includes all two-body interactions [10]. For simplicity, we neglect the interaction between identical fermions and assume the one between dissimilar fermions to be $v(r) = D\,\mathrm{sech}^2(r/r_0)$, where r is the interatomic distance and D is tuned to produce the desired a. We choose the atomic mass m and effective range $r_0 = 181$ a.u. [11] to be those of ^{40}K. The eigenvalues and eigenfunctions of $\hat{H}_{\rm ad}$, namely, the hyperspherical potentials $U_\nu(R)$ and channel functions $\Phi_\nu(R;\Omega)$, determine the effective potentials and nonadiabatic couplings in Eq. (1): $W_{\nu\nu} = U_\nu - Q_{\nu\nu}/2\mu$ and $W_{\nu\nu'} = -[P_{\nu\nu'}d/dR + Q_{\nu\nu'}]/2\mu$, where $P_{\nu\nu'} = \langle\Phi_\nu|d/dR|\Phi_{\nu'}\rangle$ and $Q_{\nu\nu'} = \langle\Phi_\nu|d^2/dR^2|\Phi_{\nu'}\rangle$. We find $\Phi_\nu(R;\Omega)$ variationally by expanding in exact eigenfunctions of Eq. (2) at large *and* small R [8]. At ultracold energies the convergence of the scattering observables with respect to the number of basis functions is surprisingly fast [8].

However, including higher-order correlations that describe dimer-atom-atom and four free atom configurations is crucial for *accurately* describing scattering processes at *any* collision energy. We find that for $R \lesssim a$ the strongest contribution to the probability density of the dimer-dimer channel function comes from dimer-atom-atom-like configurations. Figure 1 shows a graphical representation of this channel function in terms of the internal configuration angles ϕ_1, ϕ_2, and ϕ_3. The four surfaces explicitly illustrate the fourfold symmetry ($S_2 \otimes S_2$) of the fermionic problem. The long midlines of the surfaces correspond to the interaction valleys where two dissimilar fermions are in close proximity while the wide parts loosely represent the larger phase space explored by dimer-atom-atom-like configurations.

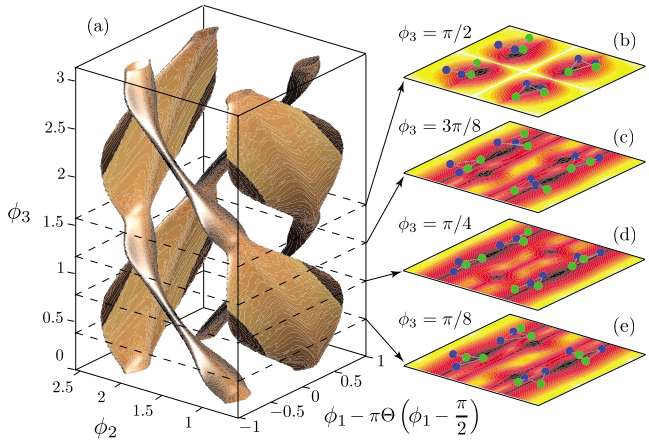

FIG. 1. (Color online) Analysis of the probability density integrated over the hyperangles θ_1 and θ_2 at $R = 0.41a$ is shown. (a) An isosurface of the probability density at $|\Phi(R;\Omega)|^2 = 0.1|\Phi(R;\Omega)|^2_{\rm max}$ for the dimer-dimer channel is shown. The darker (lighter) colors correspond to a more (less) linear configuration for the four-particle system. $\Theta(x)$ is the unit-step function. (b)–(e) show density plots for fixed values of ϕ_3. The darker regions represent higher probabilities for which planar configurations are shown to illustrate the most probable four-body geometry at selected points.

Figure 2(a) shows the hyperspherical potentials for $a = 125r_0$ showing the full energy landscape with the four-body thresholds for dimer-dimer ($FF'+FF'$), dimer-atom-atom ($FF'+F+F'$), and four atom ($F+F'+F+F'$) collisions. Notice that the four-body potential associated with dimer-dimer collisions is repulsive for $R < a$, indicating that zero-energy dimer-dimer elastic scattering must be qualitatively similar to scattering by a hard sphere of radius a, i.e., $a_{\rm dd}(0) \propto a$. Although a clear and qualitative picture emerges from the four-body potentials alone, we in practice extract

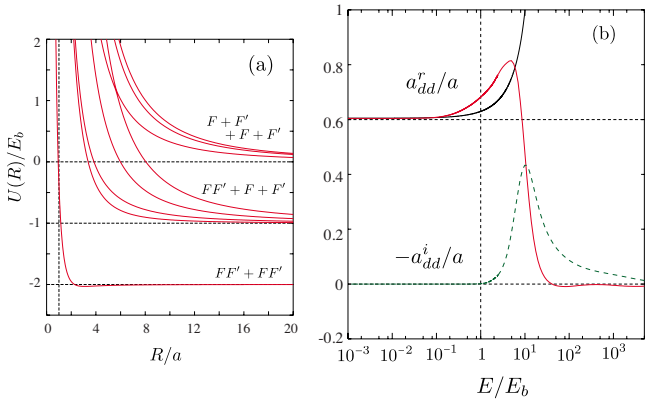

FIG. 2. (Color online) (a) Several four-fermion hyperspherical potentials attached to all relevant breakup thresholds are shown. (b) The energy-dependent elastic (red solid line) and inelastic (green dashed line) parts of $a_{\rm dd}$ [Eq. (3)] are shown. For energies $E \ll E_b$ we find $a^r_{\rm dd} = 0.605(5)a$ [4], while for $E_{\rm col} \approx E_b$ finite-energy corrections strongly affect $a_{\rm dd}$. Solid black line: $a_{\rm dd}$ using the effective range expansion [12].

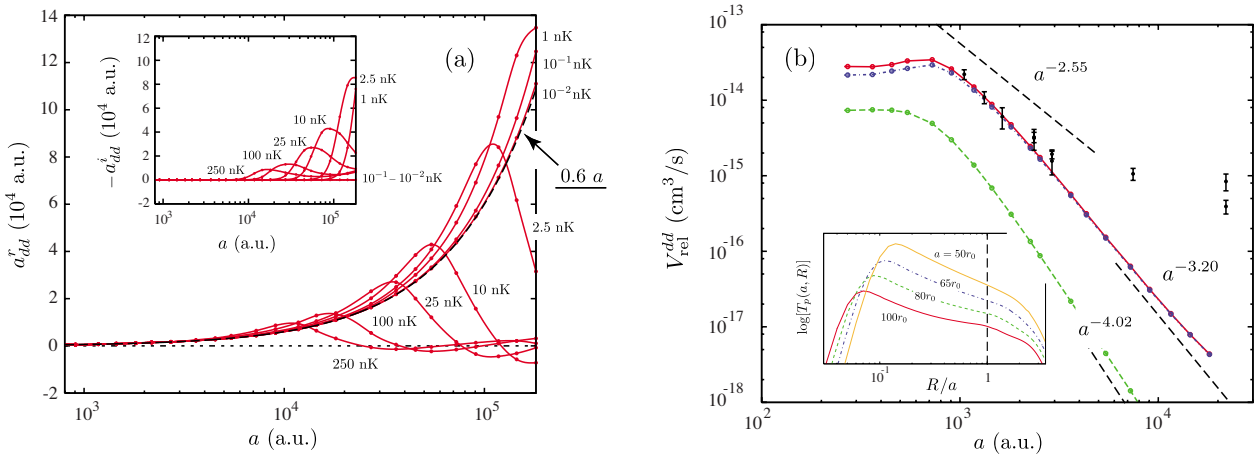

FIG. 3. (Color online) (a) The scattering length dependence of a^r_{dd} and a^i_{dd} (inset) at fixed collision energies is shown. At any nonzero collision energy a_{dd} deviates from the zero-energy prediction (black dashed line) as $a\to\infty$ and strong contributions from molecular dissociation, a^i_{dd}, occur. (b) The dimer-dimer relaxation rate, V^{dd}_{rel}, is shown versus a. The solid line is the total V^{dd}_{rel} and the dashed and dot-dashed lines are contributions from different decay pathways (see text). For intermediate a, we reproduce both experimental data [7] (filled circles) and the $a^{-2.55}$ scaling law [4] while deviating from that for larger a. Inset: we show T_p as a function of R for $a=100$, 80, 65, and $50r_0$ (red, green dashed, blue dot-dashed, and orange lines, respectively).

scattering observables from coupled-channel solutions to Eq. (1). We define the energy-dependent dimer-dimer scattering length, $a_{dd}(E_{col})$, in terms of the complex phase shift obtained from the corresponding S-matrix element [$S_{dd,dd}=\exp(2i\delta_{dd})$]

$$a_{dd}(E_{col}) = -\frac{\tan\delta_{dd}}{k_{dd}} = a^r_{dd}(E_{col}) + ia^i_{dd}(E_{col}). \qquad (3)$$

Here, $k^2_{dd}=2mE_{col}$, $E_{col}=E+2E_b$ is the collision energy, and a^r_{dd} and $a^i_{dd}<0$ are the real and imaginary parts of a_{dd}, representing elastic and inelastic contributions [6].

Figure 2(b) shows a^r_{dd} and a^i_{dd} for $a=125r_0$. For energies $E_{col}\ll E_b$ we find that $a_{dd}(0)=0.605(5)a$ in agreement with Refs. [4,12], while for $E_{col}\lesssim E_b$, although molecular dissociation is still not allowed, i.e., $a^i_{dd}=0$, we obtain strong corrections to the zero-energy result. At these energies, an effective range expansion, $a^{-1}_{dd}(E_{col})=a^{-1}_{dd}(0)-\frac{1}{2}r_{dd}k^2_{dd}$ where $r_{dd}=0.13a$ [12], is accurate over a small range but quickly fails to reproduce our results [see black solid line in Fig. 2(b)]. For $E_{col}\gtrsim E_b$, the channels for molecular dissociation become open, leading to strong inelastic contributions to $a_{dd}(E_{col})$, as parametrized by a^i_{dd}. Our results indicate that both a^r_{dd} and a^i_{dd} are universal functions of energy and scattering length, i.e., insensitive to the details of the short-range physics, which should extend up to $E_{col}\ll 1/mr^2_0$ in the absence of deeply bound states. Due to the small number of basis functions used in these calculations, our results for $E_b\ll E_{col}\ll 1/(mr^2_0)$ are not fully converged, but we expect their qualitative behavior, i.e., the sharp decease in $a_{dd}(E_{col})$, to persist.

Figure 3(a) demonstrates that when approaching the Feshbach resonance ($a\to\infty$) at any finite collision energy, molecular dissociation becomes increasingly more important and a^r_{dd} substantially deviates from the zero-energy predictions [black dashed line and inset in Fig. 3(a)]. As $a\to\infty$, $E_b\propto 1/a^2$ becomes extremely small and such finite-energy effects [see Fig. 2(b)] are relevant even at ultracold energies. Therefore, the molecular binding energy E_b, or equivalently $a_c=1/\sqrt{2\mu_{2b}T}$, defines the range beyond which (i.e., $a>a_c$) deviations from the zero-energy predictions can be observed. Perhaps more importantly, it specifies a regime beyond which molecular dissociation can lead to a long-lived atom-molecule mixture [13,14], where dimers are continuously converted to atoms and vice versa, i.e., $FF'+FF'\leftrightarrow FF'+F+F'$. Further, this indicates that the underlying physics of the strongly interacting regime may fundamentally depend on temperature. Values for a_c at 100 nK are 7000 a.u. for ^{40}K and 17 000 a.u. for ^{6}Li, and therefore the finite-energy effects above can become experimentally relevant [2].

We also study vibrational relaxation due to dimer-dimer collisions. We verify the suppression of the relaxation rate as $a\to\infty$, however, with a different a dependence than $a^{-2.55}$ predicted in Ref. [4]. In Ref. [4] it was assumed that the main decay pathway for relaxations is a purely three-body process and requires only three atoms to be enclosed at short distances. Therefore, it *neglects* the effects of the interaction with the fourth atom. Here, however, we analyze such effects and find that it strongly influences the suppression of relaxation. In our calculations we express the inelastic transitions probability $T_p(a,R)$ in terms of the probability of having three atoms at short distances as a function of the distance $\approx R$ of the fourth atom from the collision center [15]. We calculate T_p from our fully coupled-channel solutions and effective potentials [see Figs. 1 and 2(a)], and our results are shown in the inset of Fig. 3(b).

In our model the relaxation rate is simply proportional to the transition probability $T_p(a,R)$. It is interesting note that our formulation allows for the analysis of different decay pathways. For instance, at short distances, $R\approx r_0$, T_p describes inelastic transitions in which *all* four atoms are involved in the collision process. At large distances, $R/a\gg 1$, T_p describes the decay pathway where *only* three atoms par-

ticipate in the collision, akin to the process studied in Ref. [4]. We note, however, that for values of R up to $R \approx 5a$ the scaling law for relaxation depends strongly on R/a and greatly deviates from the $a^{-2.55}$ scaling. In order to take into account inelastic processes for all values of R we define an effective transition probability by integrating $T_p(a,R)$ over R [15]. Our results for the relaxation rate, $V_{\mathrm{rel}}^{\mathrm{dd}}$, are shown in Fig. 3(b) where the red solid line is obtained by integrating T_p from $R=2r_0$ up to $10a$ [16], giving an apparent scaling law of $a^{-3.20\pm0.05}$. The dot-dashed and dashed lines are obtained from integrating T_p from $R=2r_0$ to $5r_0$ and from $R=5r_0$ to $10a$, which yields scaling laws of $a^{-4.02}$ and $a^{-3.20\pm0.05}$, respectively, "separating" the contributions from the decay pathways in which four and three atoms participate in the collision process. The amplitudes for each of these contributions, however, are disconnected as they depend on the details of the four- and three-body short-range physics. In contrast, the amplitudes for the $a^{-3.20}$ and $a^{-2.55}$ processes are governed by the same three-body physics. As a result, the fact that we do not observe the $a^{-2.55}$ scaling implies that it is not important for the range of a used here. The amplitude for the process which leads to the $a^{-2.55}$ scaling is exponentially suppressed owing to the unfavorable overlap of the dimers' wave function [see inset of Fig. 3(b)]. In fact, for our largest values of a, it is already apparent that in the very large a limit the rate deviates from $a^{-3.20}$, however, to a behavior different than $a^{-2.55}$ [15].

Figure 3(b) rescales our results for $V_{\mathrm{rel}}^{\mathrm{dd}}$ by an overall constant chosen to fit the experimental data for ^{40}K at a temperature of 70 nK (Regal *et al.* [7]). We note, however, that between $a=1000$ and 3000 a.u. [17], our results agree with both the experimental data and the $a^{-2.55}$ scaling law, approaching our predicted scaling law $a^{-3.20}$ only for larger values of a. This change in behavior of $V_{\mathrm{rel}}^{\mathrm{dd}}$ originates in the finite range of our model, which represents physics beyond the zero-range model of Ref. [4] where the $a^{-2.55}$ scaling applies for all a.

In summary, we have calculated the energy-dependent complex dimer-dimer scattering length, $a_{\mathrm{dd}}(E_{\mathrm{col}})$, by solving the four-body Schrödinger equation in the adiabatic hyperspherical representation. Our results demonstrate that for experimentally relevant temperatures and scattering lengths the elastic and inelastic contributions of a_{dd} are equally important. We show that molecular dissociation plays an important role and suggest that the many-body behavior in the strongly interacting regime might be significantly altered at finite temperature. Our results also demonstrate a stronger suppression for dimer-dimer relaxation, compared to that obtained in Ref. [4], while remaining consistent with experimental data.

The authors would like to acknowledge D. S. Jin's group for providing their experimental data, J. von Stecher and D. S. Petrov for fruitful discussions, and the W. M. Keck Foundation for providing computational resources. This work was supported by the National Science Foundation.

[1] D. M. Eagles, Phys. Rev. **186**, 456 (1969); A. J. Leggett, J. Phys. (Paris), Colloq. **41**, C7-19 (1980); M. Holland, S. J. J. M. F. Kokkelmans, M. L. Chiofalo, and R. Walser, Phys. Rev. Lett. **87**, 120406 (2001); E. Timmermans *et al.*, Phys. Lett. A **285**, 228 (2001); Y. Ohashi and A. Griffin, Phys. Rev. Lett. **89**, 130402 (2002).

[2] C. Chin *et al.*, Science **305**, 1128 (2004); T. Bourdel *et al.*, Phys. Rev. Lett. **93**, 050401 (2004); M. Bartenstein *et al.*, *ibid.* **92**, 120401 (2004); C. A. Regal, M. Greiner, and D. S. Jin, *ibid.* **92**, 040403 (2004); M. W. Zwierlein *et al.*, *ibid.* **92**, 120403 (2004); G. B. Partridge, K. E. Strecker, R. I. Kamar, M. W. Jack, and R. G. Hulet, *ibid.* **95**, 020404 (2005); M. Bartenstein *et al.*, *ibid.* **92**, 203201 (2004); J. Kinast, S. L. Hemmer, M. E. Gehm, A. Turlapov, and J. E. Thomas, *ibid.* **92**, 150402 (2004); M. Greiner, C. A. Regal, and D. S. Jin, *ibid.* **94**, 070403 (2005); M. W. Zwierlein *et al.*, Nature (London) **435**, 1047 (2005).

[3] P. Pieri and G. C. Strinati, Phys. Rev. B **61**, 15370 (2000).

[4] D. S. Petrov, C. Salomon, and G. V. Shlyapnikov, Phys. Rev. Lett. **93**, 090404 (2004); Phys. Rev. A **71**, 012708 (2005).

[5] M. J. Wright *et al.*, Phys. Rev. Lett. **99**, 150403 (2007).

[6] J. L. Bohn and P. S. Julienne, Phys. Rev. A **56**, 1486 (1997); R. C. Forrey, N. Balakrishnan, V. Kharchenko, and A. Dalgarno, *ibid.* **58**, R2645 (1998).

[7] J. Cubizolles, T. Bourdel, S. J. J. M. F. Kokkelmans, G. V. Shlyapnikov, and C. Salomon, Phys. Rev. Lett. **91**, 240401 (2003); K. E. Strecker, G. B. Partridge, and R. G. Hulet, *ibid.* **91**, 080406 (2003); C. A. Regal, M. Greiner, and D. S. Jin, *ibid.* **92**, 083201 (2004).

[8] Nirav P., Mehta, Seth T. Rittenhouse, José P. D'Incao, and Chris H. Greene, e-print arXiv:0706.1296.

[9] V. Aquilanti and S. Cavalli, J. Chem. Soc., Faraday Trans. **93**, 801 (1997); A. Kuppermann, J. Phys. Chem. A **101**, 6368 (1997).

[10] We omit all reference to the Euler angles because this study treats only the dominant partial wave $J^{\pi}=0^{+}$, where J is the total orbital angular momentum and π is the parity quantum number.

[11] V. V. Flambaum, G. F. Gribakin, and C. Harabati, Phys. Rev. A **59**, 1998 (1999). The value for r_0 is obtained from the expression $r_0=2^{1/2}3^{-1}\Gamma(\frac{1}{4})\Gamma(\frac{3}{4})^{-1}(mC_6)^{1/4}$ [Eq. (24)] at resonance.

[12] J. von Stecher, Chris H. Greene, and D. Blume, Phys. Rev. A **76**, 053613 (2007); **77**, 043619 (2008). a_{dd} in these works is calculated to an accuracy similar to our present value.

[13] S. Jochim *et al.*, Phys. Rev. Lett. **91**, 240402 (2003).

[14] Y. I. Shin, A. Schirotzek, C. H. Schunck, and W. Ketterle, Phys. Rev. Lett. **101**, 070404 (2008).

[15] See EPAPS Document No. E-PLRAAN-79-R13902 for a more detailed description of our model for dimer-dimer relaxation. For more information on EPAPS, see http://www.aip.org/pubservs/epaps.html.

[16] We have found that integrating T_p from $R=2r_0$ up to $10a$ is enough to ensure that contributions for $R<2r_0$ and $R>10a$ are negligible.

[17] The experimental data for $a>3000$ a.u. were taken in the regime where the molecular size is expected to be larger than the interparticle spacing, which prohibits a proper comparison to our results.